Energetics but not development is impacted in coral embryos exposed to ocean acidification

Chille EE [1*], Strand EL [1], Scucchia F [2,3], Neder M [2,3], Schmidt V [4], Sherman MO [1], Mass T [2,5], Putnam HM [1]

Affiliations:

[1] Department of Biological Sciences, University of Rhode Island, Rhode Island, USA

[2] Department of Marine Biology, The Leon H. Charney School of Marine Sciences, University of Haifa, Haifa, Israel

[3] The Interuniversity Institute of Marine Sciences, Eilat, Israel

[4] Yale School of Medicine, Yale University, Connecticut, USA

[5] Morris Kahn Marine Research Station, The Leon H. Charney School of Marine Sciences, University of Haifa, Sdot Yam, Israel

* corresponding author: Erin Chille, erin_chille@uri.edu

Keywords: DESeq2, MZT, maternal provisioning, RNAseq

Summary statement

This developmental time series tracks the physiological and transcriptomic outcomes of early coral development under ambient pH (pH 7.8), and two low pH conditions (pH 7.6 and 7.3).

Abstract

In light of the chronic stress and mass mortality reef-building corals face under climate change, it is critical to understand the processes essential to reef persistence and replenishment, including coral reproduction and development. Here we quantify gene expression and size sensitivity to ocean acidification across a set of developmental stages in the rice coral, *Montipora capitata*. Gametes and then embryos and swimming larvae were exposed to three pH treatments ranging from 7.8 (Ambient), 7.6 (Low) and 7.3 (Xlow) from fertilization to 9 days post-fertilization. Embryo development and size, planula volume, and stage-specific gene expression were compared between treatments at each stage to determine the effects of acidified seawater on early development. While there was no measurable size differentiation between fertilized eggs and embryos at the prawn chip stage exposed to ambient, low, and extreme low pH, early gastrula and planula raised in reduced pH treatments were significantly smaller than those raised in ambient seawater, suggesting an energetic cost to developing under low pH. However, no differentially expressed genes emerged between treatments at any time point, except swimming larvae. Larvae from pH 7.6 showed upregulation of genes involved in cell division, regulation of transcription, lipid metabolism, and oxidative stress in comparison to the other two treatments, and smallest sizes in this treatment. While low pH appears to increase energetic demands and trigger oxidative stress, the developmental process is robust to this at a molecular level, with swimming larval stage reached in all pH treatments.

Introduction

As anthropogenic carbon dioxide (CO_2) levels continue to rise and contribute to global climate change (Bindoff et al., 2019), approximately one-third of atmospheric CO_2 is also being absorbed by the surface ocean (Sabine et al., 2004). Increasing concentrations of CO_2 in the surface ocean leads to ocean acidification (OA) through a shift in the chemical equilibrium of carbon in seawater (Sabine et al., 2004) that reduces ocean pH and the availability of carbonate ions (Caldeira and Wickett, 2003) for calcium carbonate formation. The absorption of

atmospheric CO_2 by the surface ocean has already driven a 0.1 unit decrease in oceanic pH, which is projected to decrease by an additional 0.036–0.042 or 0.287–0.29 units by the year 2100 under best (RCP 2.6) and worst-case (RCP 8.5) scenarios, respectively (Bindoff et al., 2019).

A growing body of studies has reported negative effects of reduced seawater pH on marine organisms. OA can negatively impact biomineralizing marine taxa that build calcium carbonate shells and skeletons (Doney et al., 2009; Kroeker et al., 2010). Coral reefs are one marine system threatened by OA as reef corals are ecosystem engineers, building skeletons that generate the 3-dimensional complexity and thus creating habitat for an entire ecosystem. Corals are also threatened by a variety of additional anthropogenic stressors such as marine heatwaves, pollution, sedimentation, and disease (Harvell et al., 2002; Hughes et al., 2017; Maynard et al., 2015). While adult organism calcification has been the primary response challenged by OA, less is known about the impact of OA on embryonic development, despite concerns that sensitivity to environmental stressors during early development can present a bottleneck for species persistence in a changing ocean (Byrne, 2012; Przeslawski et al., 2015). These early life stages are crucial for the resilience of species given their role in repopulating and replenishing existing populations (Adjeroud et al., 2017; Ritson-Williams and Arnold, 2009).

OA can affect multiple early developmental processes in corals and other marine invertebrates. Specifically, lower pH impacts sperm motility (Albright, 2011; Havenhand et al., 2008; Morita et al., 2010), fertilization success (Albright, 2011; Albright and Mason, 2013; Albright et al., 2010; Byrne, 2012; Han et al., 2021; Havenhand et al., 2008; Kurihara and Shirayama, 2004), larval settlement (Albright, 2011; Albright and Langdon, 2011; Albright et al., 2010), and post-settlement growth (Albright and Langdon, 2011; Albright et al., 2008; Albright et al., 2010; Scucchia et al., 2021a). In corals, decreased fertilization efficiency has been observed, which may be explained by decreased sperm flagellar motility and increased polyspermy under low pH (Albright and Mason, 2013; Albright et al., 2010). Low pH is also correlated with metabolic depression in many coral species (Moya et al., 2012; Moya et al., 2015; Nakamura et al., 2011; Putnam et al., 2013), which may explain observations of delayed development, smaller embryo/larval volume, and reduced post-settlement growth in corals developing in acidified conditions (Albright and Langdon, 2011; Nakamura et al., 2011; Rivest and Hofmann, 2014;

Yuan et al., 2018). The increased energetic costs of maintaining homeostatic processes under disrupted acid-base balances and ionic gradients can additionally slow development and reduce growth of marine invertebrate larvae and recruits (Albright and Langdon, 2011; Byrne, 2012; Przeslawski et al., 2015; Timmins-Schiffman et al., 2013). For example, low pH is correlated to delayed cleavage (Foo et al., 2012), smaller larvae (Kelly et al., 2013), and depressed metabolism (O'Donnell et al., 2010) during the early development of sea urchins. Developmental delays (Barton et al., 2012; Timmins-Schiffman et al., 2013) and decreases in fertilization rate (Barros et al., 2013; Parker et al., 2009; Parker et al., 2010), hatching success (Barros et al., 2013; Gazeau et al., 2010; Van Colen et al., 2012), larval survival (Barros et al., 2013; Van Colen et al., 2012) and larval size, (Barros et al., 2013; Barton et al., 2012; Van Colen et al., 2012) have also been observed in bivalves under low pH. These compounding effects of low pH and co-occurring stressors can present a major life history bottleneck, leading to downstream effects on the resilience of marine invertebrate species (Byrne, 2012; Byrne and Przeslawski, 2013).

Most studies examining the effects of OA on coral development thus far have focused primarily on fertilization, settlement, and post-settlement growth, with less of a focus on embryonic development. In many species, embryogenesis represents a critical window in development during which time embryos are particularly sensitive to environmental fluctuations outside of the expected range (Byrne, 2012; Byrne et al., 2009; Dahlke et al., 2020; Ericson et al., 2010; Ericson et al., 2012; Foo et al., 2012; Przeslawski et al., 2015). Several studies have implicated the loss of maternal defenses during the maternal-to-zygotic transition (MZT) as playing a role in increased environmental sensitivity during this period (Dahlke et al., 2017; Dahlke et al., 2020; Ericson et al., 2012; Foo et al., 2012; Przeslawski et al., 2015). The MZT describes the developmental reprogramming of gene expression from maternal to zygotic regulation (Tadros and Lipshitz, 2009; Vastenhouw et al., 2019). During the MZT, the maternally-provided gene products that regulate early development and protect embryos from expected stressors are degraded as zygotic transcription activates and intensifies (Tadros and Lipshitz, 2009; Vastenhouw et al., 2019). Higher mortality in response to environmental perturbations has been observed during this transition in fish gastrula (Dahlke et al., 2017; Dahlke et al., 2020), sea

urchin blastula/gastrula (Ericson et al., 2012; Foo et al., 2012), and several other marine invertebrates (Przeslawski et al., 2015).

Maternal mRNA provisioning and the timing of the MZT in reef-building corals, thus far, have only been investigated in the Hawaiian rice coral, *Montipora capitata* (Chille et al., 2021). Under ambient conditions, the maternal mRNA complement in *M. capitata* eggs primarily provide housekeeping functions, including cell cycle, biosynthesis, transcription, signaling, and protein processing (Chille et al., 2021; Van Etten et al., 2020). However, DNA repair mechanisms, which may protect early embryos from ultraviolet (UV) radiation and reactive oxygen species (ROS), are also over-represented in the *M. capitata* maternal mRNA complement of eggs (Chille et al., 2021). As of yet, the maternal mRNA complement in reef-building corals has not been assessed under stressful conditions. However, based on timing of the MZT in *M. capitata* (Chille et al., 2021), and general developmental gene expression studies in *Acropora millepora* (Strader et al., 2018), *Acropora digitifera* (Reyes-Bermudez et al., 2016), and *Nematostella vectensis* (Helm et al., 2013), coral embryos may be most sensitive to stress during early gastrulation (between 9 and 14 hours post-fertilization; hpf), when a large portion of maternal transcripts are degraded and zygotic transcription begins.

Previous transcriptomic examinations of pH-stress during coral embryonic development have been done on aposymbiotic species (Acropora; Strader et al., 2018) and on post-settlement stages after the completion of the MZT (Moya et al., 2012; Scucchia et al., 2021a). Here, we use *Montipora capitata*, a hermaphroditic broadcast spawner with vertical symbiont transmission that is endemic to the Hawaiian archipelago (Heyward, AJ, 1986; Padilla-Gamiño and Gates, 2012) to examine the embryonic sensitivity to OA in the context of the MZT. In this study, we examined the physiological and transcriptomic outcomes of early coral development in five life stages from fertilization until the “completion” of early coral development (i.e. fully-developed larvae) under pH 7.8 (ambient), and two low pH conditions (7.6 and 7.3). This time series allows us to determine sensitivity to and phenotypic consequences of OA during and after the MZT.

Materials and Methods

Specimen collection

Montipora capitata egg-sperm bundles were collected under the Department of Land & Natural Resources Special Activity Permit 2018-50 from the reef adjacent to the Hawaiʻi Institute of Marine Biology, Coconut Island, Kāneʻohe Bay, Oʻahu Hawaiʻi (21°25'58.0"N 157°47'24.9"W) at ~21:00 on June 13, 2018. After collection, egg-sperm bundles were allowed to break apart. Eggs were separated from the sperm and rinsed 3 times with 0.2 uM filtered seawater, then snap-frozen and stored at -80 °C in ~300 uL aliquots.

Experimental set-up

Fertilization and early development occurred in nine 1.6 L conicals flow-through tanks set to pH 7.8 (ambient), pH 7.6, and pH 7.3 pH (n=3 conical tanks per treatment, Fig.1A). At 22 hpf, the embryos were transferred to replicate 118 ml bins with 152µm plankton mesh bottoms floating in 74L glass tanks (n=3 bins per tank, 2 tanks per treatment; Fig. 1B) Treatments were designed to reflect future ocean acidification conditions in coastal embayments (Jury et al., 2013; Shaw et al., 2016) including daily fluctuations naturally occurring in Kāneʻohe Bay, Hawaiʻi (Drupp et al., 2011). All treatments were controlled by a pH-stat feedback system in one header tank per treatment. Header tank conditions were continuously monitored using a Neptune Apex Reef Aquarium set-up (Energy Bar 832; Controller Base Unit; PM1 pH/ORP Probe Module; Extended Life Temperature Probe; pH Probe), and 99.99% food-grade CO_2 was injected into the header tanks with gas flow solenoids (Milwaukee MA955) using inline venturi injectors (Forfuture-go G1/2 Garden Irrigation Device Venturi Fertilizer Injector) in a pressure driven line connected to a circulating pump (Pondmaster Pond-mag Magnetic Drive Water Pump Model 5) in each header tank (Fig. 1A). Water flow was delivered at a maximum potential flow rate of 7.57 liters per hour by 1.9 LPH (0.5 gallons per hour) Pressure Compensating Drippers for a conical turnover rate of once every ~50 minutes, and once every ~23 hours for a 74 L tank. The average light intensity, 96±8.823 mean±sem umol m^{-2} s^{-1} (n=24), was measured using a handheld PAR sensor (Underwater Quantum Flux Apogee instruments - Model MQ-510; accuracy = ±4%).

Temperature, salinity, and pH were measured three times daily in each treatment tank using a handheld digital thermometer (Fisherbrand Traceable Platinum Ultra-Accurate Digital

Thermometer, accuracy = ±0.05 °C, resolution = 0.001°) and a portable multiparameter meter (Thermo Scientific Orion Star A series A325; accuracy = ±0.2 mV, 0.5% of psu reading, resolution = 0.1 mV, 0.01 psu) with pH and conductivity probes (Mettler Toledo InLab Expert Pro pH probe #51343101; Orion DuraProbe 4-Electrode Conductivity Cell Model 013010MD), respectively (Table 1). Temperature and pH probes were calibrated using Tris (Dickson Laboratory Tris Batch 27, Bottles 70, 75, 167, 245, and 277) standard calibrations. Total alkalinity (µmol kg^{-1} seawater) was measured from water samples daily using an automated titrator (Mettler Toledo T50) and hydrochloric acid (Dickson Laboratory Titrant A3), and certified reference material (Dickson Laboratory CO_2 CRM Batch 149) was used as a quality control standard. Carbonate chemistry parameters (pH, CO_2, pCO_2, HCO_3, CO_3, dissolved inorganic carbon, total alkalinity, and aragonite saturation) were calculated from total alkalinity measurements using SEACARB v3.0.11 (Gattuso et al., 2015) in RStudio (Table 1 and Table S1) using Kf from (Perez and Fraga, 1987), K1 and K2 from (Lueker et al., 2000) and Ks from (Dickson, 1990). Seawater pH was calculated on the total scale (Dickson et al., 2007); SOP6a), using the gas constant (8.31447215 J K^{-1} mol^{-1}) and the Faraday constant 96485.339924 coulombs mol^{-1}).

Sample collection and preservation

Physiological and molecular samples were taken immediately upon breakup of egg-sperm bundles and at five timepoints following transfer to experimental conditions (Fig. 1). Sampling times represent visually-distinct developmental stages including fertilized embryo (1-hr post-fertilization), cleavage (4-hr post-fertilization), prawn chip (9-hr post-fertilization), early gastrulation (14-hr post-fertilization), and planula (9-d post-fertilization). Physiological samples (~100-200 embryos or larvae per replicate) were preserved in 500 µL 25% zinc buffered formalin in 0.2µm filtered seawater, and stored at 4°C. Molecular samples (300 µL of embryos per replicate) were snap-frozen in liquid nitrogen and stored at -80°C.

Embryo development and growth

Stereomicroscope images of fixed samples were analyzed for blastomere number at 4 hpf (cleavage stage), and for maximum length and perpendicular width of the unfertilized eggs, gastrula, and planula using ImageJ (Schneider et al., 2012). Cell division stage was assessed in

cleavage-stage samples with 82 to 282 embryos/sample (n=3 replicate samples treatment^{-1}). Embryos were classified as "one cell," "two cells," "four cells," or "greater than four cells." The percentage of embryos at each stage of cell division was then calculated for each sample to examine potential variation in developmental timing between treatments. Volume of unfertilized eggs (n=50), fertilized embryos (n=225), early gastrula (n=200), and planulae (n=150) was calculated using the equation for an oblate ellipse: $V = \frac{4}{3}\pi a b^2$ in which V is equal to volume, a is the half of maximum width and b is the half maximum length to examine differences in size between treatments through early development.

All statistical analyses for morphological data were performed in RStudio (v1.3.959; RStudio Team, 2020), using R version 4.0.2 (R Core Team, 2013). A beta regression model was used to analyze variation in the proportion of cells at each cleavage stage and treatment. Additionally, a one-way nested ANOVA analysis tested the effect of tank on embryo and planula size wherein tank ID was nested within treatment. After determining that tank effects were insignificant ($P > 0.05$), one-way ANOVA analysis was used to test for the effect of treatment on fertilized embryo, gastrula, and planula volume. Post hoc Tukey HSD tests were conducted when the effect of treatment was significant ($P < 0.05$). Data were visually examined for normal distribution and equal variance. The dependent variable was square-root transformed for the gastrulation and planula life stages in order to meet statistical assumptions prior to ANOVA analysis. Data points for these life stages were back-transformed for visualization in Figure 2.

RNA extraction, sequencing, and processing

To extract RNA, molecular samples were digested at 55°C in 300 µl of DNA/RNA Shield (Zymo Research, Irvine, CA, USA) for two to three-and-a-half hours and centrifuged at 2200 RCF for one minute to separate the remaining solids. Total RNA was extracted from each supernatant with the Zymo Quick-DNA/RNA™ Miniprep Plus Kit (Zymo Research, Irvine, CA, USA) following the manufacturer's protocol for tissue samples. RNA was quantified (ng/µL) with a ThermoFisher Qubit Fluorometer and quality was assessed using the Eukaryote RNA analysis on the Agilent TapeStation 4200 System. Total RNA samples were then sent to Genewiz (South Plainfield, New Jersey, USA) for library preparation and sequencing. cDNA libraries were constructed following the TruSeq Stranded mRNA Sample Preparation protocol

(Illumina, San Diego, CA, USA) and sequenced on a HiSeq instrument targeting 15 million reads per sample. Quality trimming, alignment, and assembly were conducted as described in (Chille et al., 2021). In short, sequences were filtered for quality by applying a five base pair sliding window to remove reads with an average quality score less than 20, and retaining sequences with quality scores greater than or equal to 20 in at least 90% of bases and sequence length greater than or equal to 100 bases. Trimmed reads were then aligned to an *M. capitata* reference assembly (Shumaker et al., 2019) using HISAT2 in the stranded paired-end mode (Kim et al., 2019), and assembled with StringTie in the stranded setting (v2.1; Pertea et al., 2015). Finally, the StringTie *prepDE* python script (Pertea et al., 2015) was used to generate a gene count matrix from the resulting GFFs (Pertea et al., 2015).

Host gene expression analyses

Experiment-wide patterns in gene expression were assessed with a principal components analysis (PCA). First, the full gene count matrix was pre-filtered improve to remove low-coverage counts with the Genefilter (v1.70.0; Gentleman et al., 2020) function *pOverA* to exclude genes where fewer than 2 out of 41 (~0.0488) samples had counts under 10 (pOverA 0.0488, 10). A value of p=0.0488 was chosen under the assumption that due to the MZT, a gene count of zero likely represents a true zero because some genes in *M. capitata* embryos may not be activated at until the onset of gastrulation or later (Chille et al., 2021). Then, counts were transformed with DESeq2's (v1.28.1) variance stabilizing transformation (vst) function (Love et al., 2014a) after confirming that all size factors were less than 4. Finally, the vst-transformed counts were used for PCA to visualize expression results for all filtered genes. The DESeq2 *plotPCA* function was used to generate a PCA of all samples based on sample-to-sample distance. All gene expression analyses were performed in RStudio (v1.3.959; RStudio Team, 2020), using R version 4.0.2 (R Core Team, 2013).

PCA and differential gene expression analysis with DESeq2 were used to assess within-stage differences in expression due to treatment. As described above, genes with low overall expression were filtered using the Genefilter *pOverA* filter function (Gentleman et al., 2020). After testing a range of values from p=0.33 to p=0.9, a more conservative value of p=0.875 was chosen to prevent bias due to high duplication levels in the first four life stages where zeros

likely represent true zeros compared to the planula samples which had lower duplication. As such, we retained genes with greater than 10 counts in at least 7 out of 8 samples (pOverA 0.875, 10) for further analysis. The resulting genes were then vst-transformed using the DESeq2 *vst-transformation* function (Love et al., 2014b). PCA was conducted with the DESeq2 *plotPCA* function (Love et al., 2014b), using vst-transformed counts to calculate sample-to-sample distance. Differential expression analysis between pH treatments was then performed for each life stage using the filtered counts (pOverA 0.875, 10). Pairwise differences in gene expression between treatments were estimated using Wald model in DESeq2 (Love et al., 2014b). As DESeq2 results showed zero differentially-expressed genes (DEGs) in all treatment comparisons prior to the planula stage, only genes with padj<0.05 in the planula stage were used for further analysis. To visualize the DEGs that were shared and distinct for each treatment comparison within the planula stage, the results were summarised as a venn diagram (Fig. 4A) using the VennDiagram R package v1.6.20 (Chen and Boutros, 2011). Overall expression patterns among the planula DEG set were visualized as a heatmap using the ComplexHeatmap package v2.5.4 (Gu et al., 2016), with clustering based on differences in expression compared to the rowmean in the vst-transformed count matrix. Clusters in the heatmap are based on k-means clustering using the R package NbClust v3.0 (Malika et al., 2014) to calculate the optimal number of clusters using 30 indices.

Host gene ontology enrichment analyses

Gene ontology (GO) enrichment analysis was performed on the planula DEG set to examine the biological processes and molecular functions primarily correlated with each DEG k-means cluster. Firstly, gene ontology annotation of the *M. capitata* genome was retrieved from (Chille et al., 2021). To supplement the GO annotation for functional enrichment analysis, Kegg annotation was completed using KofamScan (v1.3.0; Aramaki et al., 2020), to retrieve Kegg terms in the eukaryote profiles database (v. April 23, 2021). GO enrichment analysis was performed on the DEGs with log2FoldChange>|1| in each k-means cluster using the R package Goseq (v1.40.0; Young et al., 2010). Subsequently, slim categories for the enriched GO terms were obtained using the *goSlim* function in the R package, GSEABase, using the generic GOslim obo database as reference (http://current.geneontology.org/ontology/subsets/goslim_generic.obo; v1.2; Ashburner et al., 2000). Finally, enriched biological process and molecular function terms

with numInCat > 5 and their associated slim categories were visualized as a heatmap using the ggplot2 *geom_tile* function (Wickham, 2011).

Symbiont transcriptome assembly and gene expression analysis

To assess correlation between pH Treatment and gene expression of Symbiodinaceae within the planula host, the symbiont transcriptomes were extracted from a *de novo*-assembled holobiont sequence library and analysed for differential expression between treatments. The holobiont transcriptome was assembled *de novo* using Trinity v2.12.0 (Grabherr et al., 2011) with the stranded 'RF' option. The 9 planula libraries were used to construct the holobiont transcriptome. The three adult *Montipora capitata* libraries from (Chille et al., 2021) were additionally used for *de novo* assembly in order to obtain a symbiont-rich library. Following assembly, completeness was assessed using BUSCO v4.0.6 (Simão et al., 2015) to detect the presence of single-copy orthologs universal to alveolata (for the symbionts) and metazoans (for the host). The host and symbiont transcriptomes were then identified from the holobiont assembly using *psytrans* (https://github.com/sylvainforet/psytrans) using *Cladocopium* C1 (Liew et al., 2016; Voolstra et al., 2015) and *Montipora capitata* (Shumaker et al., 2019) predicted proteins as references. Following host-symbiont separation, the symbiont reads were used as a reference file for the Trinity *align_assemble* perl script (Grabherr et al., 2011) using RSEM v1.3.3 (Li and Dewey, 2011) for abundance estimation and Bowtie v-1.2.1.1 as the alignment method (Langmead, 2010). Finally, the symbiont gene counts were obtained using the Trinity *abundance_estimates_to_matrix* perl script (Grabherr et al., 2011). Differential gene expression of the planula endosymbionts was carried out using the methods described for the host early life stages (see *Differential gene expression analysis*). Finally, the identities of the symbiont DEGs were determined through a local alignment search of the corresponding sequences against the NCBI non-redundant database using Blastx v2.11.0 (Altschul et al., 1997) with default parameters.

Results

Embryo development and growth

Immediately after release, prior to treatment exposure, eggs were 0.040±0.023 mm^3 (Fig. 2A). Following treatment exposure, the proportion of embryos at each cleavage stage at 4 hpf and

embryo size in the fertilized egg (1 hpf), early gastrula (14 hpf), and planula (9 days post-fertilization; dpf) samples was assessed to characterise morphological effects of developing in ambient (7.8) low (7.6) and extreme low pH (7.3) conditions. At the cleavage stage, across all treatments combined undivided cells were on average more frequent (44.77 ± 21.49%; mean ± sd) than those at the two-cell (26.51 ± 12.63%), four-cell (18.37 ± 11.23%), or greater-than-four cell stage (10.34 ± 13.40%). Beta regression analysis of the proportion of cells at each cleavage stage and treatment (Fig. 2B) shows that while there were significant differences (<0.0001) in proportions of two-, four-, and greater-than-four cell stages overall, the interaction between cleavage stage and treatment were only marginally significant (p=0.0765). Additionally, there were no significant differences between pH treatments in embryo size in the fertilized eggs (p=0.256; Fig. 2C). However, at both the early gastrula (p=0.000292; Fig. 2D) and planula stages (p=0.000109; Fig. 2E) embryos developing under ambient pH conditions were significantly larger than those developing under pH 7.6 and 7.3 conditions.

RNA sequencing, quality control, and mapping

TruSeq Illumina Stranded Paired-End (PE) sequencing resulted in 935,000,000 PE (19,392,156 mean reads/sample), with 694,800,000 PE reads (14,241,176 mean reads/sample) remaining after quality filtering and adapter removal. On average, 79.28 ± 1.95% (mean ± sem reads per sample) aligned to the reference *M. capitata* genome (Shumaker et al., 2019). Assembly quality assessment with GFFcompare showed that 63,227 genes queried from the mapped GTF files were matched to the 63,227 genes in the reference genome (Shumaker et al., 2019), with 40,883 matching intron chains, 63,218 matching loci, and zero missing elements.

Host gene expression patterns

After filtering to remove genes with fewer than 10 counts in ~4.88% of samples (i.e. the proportion representing each treatment in a given life stage), 30,271 genes remained to characterize global gene expression patterns. A principle components analysis (Fig. 3A) shows that sample-to-sample variation is primarily related to differences in life stage, with PC1 (83%) and PC2 (12%) explaining the majority of variation between life stages.

Principal components analyses computed from variation in expression of genes with greater than ten counts in seven of eight fertilized egg (10,751 genes; Fig. S1A), cleavage (12,837 genes; Fig. S1B), prawn chip (16,392 genes; Fig. S1C), early gastrula (17,669 genes; Fig. S1D), and planula (23,225 genes) samples show no differentiation between treatments until the planula stage (Fig. 3B). At the planula stage, treatment groups separate strongly along PC1 and PC2, which explain 47% and 25% of the variation between samples, respectively. Notably, ambient pH (7.8) and extreme low pH (7.3) samples cluster more similarly on PC1 than ambient and low pH (7.6) samples. However, with the exception of one ambient sample, ambient and low pH samples cluster closer than ambient and extreme low pH samples on PC2 (Fig. 3B).

Pairwise treatment comparisons within each life stage using DESeq2 (Table S2) showed zero differentially expressed genes between treatments until the planula stage. Differentiation of samples from planula raised in different treatments are supported by 5,406 DEGs between planula samples raised under the two low pH conditions relative to the ambient pH conditions. Mirroring the clustering of treatments along PC1 in Fig. 3B, a venn diagram (Fig. 4A) of shared and unique DEGs in each treatment comparison shows 2,202 DEGs between planula samples at the low and ambient pH treatments, 1,078 of which are also differentially expressed between the extreme low and low treatments. Only 66 DEGs exist between planula samples at the extreme low and ambient pH treatments. Planula DEGs were grouped into two k-means clusters based on the consensus of 11 of 30 clustering indices (Fig. 4B), with genes in Cluster 1 upregulated in the low pH treatment compared to the ambient and extreme low pH treatments, and genes in Cluster 2 exhibiting the opposite pattern (Fig. 4B).

Host gene ontology enrichment

After filtering the DEG set to retain genes with log2FoldChange>|1|, 344 DEGs remained in Cluster 1 (upregulated under low pH), and 256 remained in Cluster 2 (downregulated under low pH) for GO enrichment analysis. GO enrichment analysis revealed 39 biological processes and 31 molecular functions over-represented in Cluster 1. Biological processes overrepresented in Cluster 1 (Fig. 5A, Table S5) are primarily related to 7 slim terms, including biosynthetic process, cellular component assembly, cellular nitrogen compound metabolic process, immune

system process, lipid metabolic process, response to stress, and transport. Likewise, molecular functions overrepresented in Cluster 1 (Fig. 5B, Table S5) can be summarised by 8 slim terms, including ATPase activity, cytoskeletal protein binding, DNA binding, ion binding, kinase active, oxidoreductase activity, structural molecule activity, and transferase activity. Ion binding, in particular, includes several offspring terms under the GO category calcium ion binding. In Cluster 2, GO enrichment revealed 5 overrepresented biological processes (Fig. 5A, Table S5) represented by the slim terms biosynthetic process, immune system process, and transport, as well as 10 overrepresented molecular functions (Fig. 5B, Table S5) represented by the slim terms, ATPase activity, nucleotidyltransferase activity, peptidase activity and transmembrane transporter activity. The GO terms enriched in Cluster 1 and Cluster 2 are supported by the overrepresentation of related Kegg terms in both clusters (Table S6), such as peroxidase [K19511], Amt family ammonium transporter [K03320], cytosolic phospholipase A2 [K16342], and calreticulin [K08057] in Cluster 1 and E3 ubiquitin-protein ligase [K22754] and [histone H4]-lysine20 N-methyltransferase SETD8 [K11428] in Cluster 2.

Symbiont transcriptome assembly and gene expression

The *M. capitata* planula and adult holobiont *de novo* assembly was constructed from 698,861,565 bases, yielding 991,330 transcripts and 656,603 genes. The N50 of the holobiont assembly was 1,102, with an average contig length of 704.97 bases and a GC content of 43.7%. A BUSCO search of the holobiont assembly against the metazoan and alveolata databases for the host and symbiont showed high completeness (90.1% alveolata and 97.5% metazoan). In total, 83.37% (826,513) of transcripts from the holobiont assembly were assigned to the host and 16.63% (164,817) of transcripts were assigned to the symbiont. Finally, using the separated assemblies as reference transcriptomes for Trinity, 4.77±0.43% (mean±se) of planula sequences aligned to the symbiont, yielding 133,811 symbiont genes for differential expression analysis.

After filtering to remove reads with fewer than 10 counts in 7 out of 8 samples, 1,365 genes remained for principal components and differential expression analyses. A principle components analysis (Fig. S2A) of the symbiont samples shows large variation in gene expression between the three low pH (7.6) samples along the PC1 (28%) and PC2 (14%) axes, but the samples from the ambient pH (7.8) and extreme low pH (7.3) each cluster by treatment. Differential gene

expression analysis with DESeq2 (Table S3) revealed 12 differentially-expressed genes (DEGs) between the ambient and low treatments, 17 DEGs between the ambient and extreme low treatments, and 0 DEGs between the low and extreme low treatments. The ten symbiont genes upregulated in the low treatment compared to the ambient aligned to the histone H3 protein as well as actin and tubulin proteins, while the two downregulated genes aligned to the pre-mRNA-splicing factor ATP-dependent RNA helicase and a cell wall-associated hydrolase (Table S4). However, the seventeen symbiont genes upregulated in extreme low treatment (Table S4) compared to the ambient were primarily associated genes regulating rDNA expression, a mucin-like protein, cytochrome P450, COPB protein, as well as several hypothetical proteins.

Discussion

Limited research has been conducted so far on the effects of OA on coral embryonic development, with a primary focus on physiological processes (Chua et al., 2013a; Chua et al., 2013b), while little is known about the changes occurring at the transcriptomic level. Here we show that while acidic seawater altered the morphological development of *M. capitata* embryos, it did not drive any substantial change in gene expression until after the MZT. Early gastrula and planula developing at pH 7.6 (low) and pH 7.3 (extreme low) were significantly smaller than those developing at pH 7.8 (ambient), suggesting an energetic cost to developing under low pH. This is also supported by functional enrichment of the genes associated with cell division, regulation of transcription, lipid metabolism, and oxidative stress that are significantly upregulated in swimming larvae (9 dpf) exposed to pH 7.6. We additionally show that transcriptomically, larvae developing at pH 7.8 and pH 7.3 were more similar than those developing at pH 7.6 and hypothesize that this may be due to high CO_2 stimulation of symbiont photosynthesis at pH 7.3, which may alleviate the effects of OA on the host fitness.

The MZT under ocean acidification

While the morphological effects of low pH were apparent by the early gastrula stage (22 hpf; Fig. 2D-E), pH did not drive any substantial changes in gene expression until the larval stage, i.e., after the zygotic transcriptome has assumed autonomy (Fig. S1; Chille et al., 2021). These results suggest that the maternal-to-zygotic transition in *M. capitata* is robust to low pH. While our study does not include survivorship data, this finding is supported by other studies on OA

stress during the embryonic development of fish (Dahlke et al., 2017; Dahlke et al., 2020) and sea urchins (Ericson et al., 2012; Foo et al., 2012) that show that while early development is robust to ocean acidification, embryos are more vulnerable after the MZT. These findings support the role of maternal gene products (i.e., mRNA, proteins, transcription factors) in buffering early embryos from environmental stress (Hamdoun and Epel, 2007). In *M. capitata*, early development is likely to be influenced by maternal transcripts until 22-36 hpf, when the zygotic transcriptome exhibits the capacity for responding to stimuli (Chille et al., 2021). Seeing as a transcriptomic response to decreased pH was only apparent at the planula stage (Fig. 3b & Fig. 4), this suggests that the transcripts necessary to buffer embryonic development from OA are already expressed under ambient conditions or that embryos possess other molecular defenses, such as maternally-provisioned proteins (Hamdoun and Epel, 2007) that buffer the effects of low pH. However, maintaining homeostasis under low pH comes with an energetic cost, as indicated by the smaller sizes of embryos developing low pH. As such, while the embryonic development of *M. capitata* may be robust to ocean acidification, the energetic cost of developing under low pH may have latent effects on larval competence and recruitment (Albright, 2011).

Outcomes of developing in low pH

In our study, low pH (pH 7.6) elicited a robust transcriptomic response in planula that implicates several processes affecting energy metabolism and larval size (Fig. 2E), including biomineralization, cellular acidosis, and cellular stress response. We detail these responses below.

Several studies have found that actively calcifying larvae may be more susceptible to changes in seawater carbonate chemistry compared to non-calcifying embryos and larvae (Byrne, 2012; Przeslawski et al., 2015) by making biomineralization more chemically and energetically difficult (Ries, 2011). In the brooding coral *Stylophora pistillata*, calcium carbonate deposition is initiated during the pre-settled larval phase (Akiva et al., 2018). While mineralization was not specifically examined in our study, as nine-day-old larvae, it is likely that the planula here were at the calcifying stage. In fact, gene ontology enrichment analysis shows that genes associated with calcium ion binding and calcification, such as calreticulin, are upregulated in larvae

exposed to pH 7.6 (Table S5). Genes involved in calcium ion binding like calreticulin provide structural and cell adhesion functions that aid in the biomineralization process (Mass et al., 2016) and may be upregulated to compensate for the chemical shift in carbon equilibrium in the seawater (Comeau et al., 2018; DeCarlo et al., 2018; Zhao et al., 2020). However, upregulation of these genes in response to OA may increase energetic demand, as observed in some adult corals (Davies et al., 2016; Vidal-Dupiol et al., 2013; Scucchia et al., 2021b). This increased demand could potentiate the rapid depletion of larval lipid stores if the energy derived from their endosymbionts is insufficient to keep up with demand (Alamaru et al., 2009; Ben-David-Zaslow and Benayahu, 2000; Harii et al., 2010), ultimately decreasing larval size.

Acid-base parameters such as pH and pCO_2 are generally considered to lead to depressed metabolism through cellular acidosis, leading to alterations in cell size (Kaniewska et al., 2012; Reipschläger and Pörtner, 1996). Here, the enrichment of terms related to ATP synthesis in the genes downregulated at low pH (pH 7.6; Table S5), and lipid metabolism in the genes upregulated at low pH (pH 7.6; Table S5) suggests alteration of larval metabolism at reduced pH. Metabolism is highly interconnected with both growth and cell cycle progression (Björklund, 2019). Additionally, mitochondria play a crucial role in setting growth rates through energy generation and lipid biosynthesis (Miettinen and Björklund, 2017). In this context, alteration in metabolism at low pH might cause changes in cell size. Here, the enrichment of terms related to cell growth and cytoskeleton in the genes upregulated at low pH 7.6 (pH 7.6; Table S5) support changes in cell cycle and cell size with acidification. Cell growth-related genes such as JNK cascade and GTPase activity have been shown to change with acidification (Liew et al., 2018), and acidic cellular pH was demonstrated to alter processes such as cytoskeletal integrity (Tominaga and Barber, 1998). Such alterations in cytoskeletal integrity could explain the observed smaller size of planula that developed under reduced pH conditions.

Chronic exposure to low pH (pH 7.6) during early development also appears to elicit the onset of cellular stress and antioxidant responses. For example, GO terms enriched in planula developing at pH 7.6, including oxidative stress, immune response, superoxide metabolic process, oxidation-reduction process, and microtubule-based process (Table S5) are linked to protein domains that protect the cell from oxidative stress through oxidoreductase activity (e.g., superoxide dismutase-

like, peroxidasin-like, and FAD-linked oxidase; DeSalvo et al., 2008; DeSalvo et al., 2010; Fernandes et al., 2007; Kaniewska et al., 2012; Lesser and Farrell, 2004; Martínez, 2007; Sampayo et al., 2003; Zhao et al., 2016) and the removal of damaged cells (e.g., Toll/interleukin-1 receptor, TNF receptor-associated factor 4 (Fuchs and Steller, 2015; Linkermann and Green, 2014; Poquita-Du et al., 2019; Todgham and Hofmann, 2009; van de Water et al., 2015). Upregulation of cellular stress and antioxidant responses is consistent with stress response mechanisms documented in adult and larval corals upon exposure to multiple stressors, including low pH (Kaniewska et al., 2012), ultraviolet radiation (Lesser and Farrell, 2004), and thermal (DeSalvo et al., 2008; DeSalvo et al., 2010; Polato et al., 2013; Rosic et al., 2014), and nutrient stress (Rosic et al., 2014). Here, cellular stress and antioxidant responses may have been induced from macromolecular damage due to ROS released from the rapid peroxidation of planula lipid stores for energy use (Polato et al., 2013) or from increased ROS production by the algal endosymbiont. Notably, however, the onset of cellular stress response may also come at an energetic cost to the planula (Sokolova et al., 2012) and lead to smaller larvae by depleting maternal lipid stores.

Symbiont stimulation under high CO_2

Predicted future increase of CO_2 in seawater has been shown to stimulate the photosynthetic activity of the algal symbiont (Krief et al., 2010; Reynaud et al., 2003). Such stimulation can enhance host fitness under acidification (Guillermic et al., 2021). In this study, the enrichment of terms related to coral oxidative stress under pH 7.6 (low; Table S5) suggests increased photosynthetic activity in the endosymbiotic algae due to the higher availability of CO_2 in seawater, as observed in the endosymbionts of *Stylophora pistillata* primary polyps and adults (Scucchia et al., 2021a; Scucchia et al., 2021b). It has been hypothesized that at higher concentrations of CO_2 the stimulation of symbiont photosynthesis could prevent acidosis of the host cells, thus helping with preserving cellular acid-base homeostasis (Gibbin et al., 2014), and ultimately alleviating the effects of OA on the host fitness, as observed here in planula developing at pH 7.3. The increase in translocated photosynthates provided by the endosymbiont under this scenario could additionally supplement the larvae's diet (Harii et al., 2010), thereby decreasing consumption of endogenous lipids and the associated influx of ROS. The differential expression of housekeeping functions, including tubulin, rRNA promoter binding proteins, and

rDNA transcriptional regulator 15 in our symbiont data (Table S3) suggest to us that there is not enough endosymbiont expression coverage in the dataset to have the power to test this hypothesis. It is possible, however that due to the potential for post-transcriptional regulation of gene expression in the Symbiodiniaceae through the use of trans-splicing of spliced leader sequences (Zhang et al., 2007; Lin et al., 2010; Lin, 2011), small RNAs and microRNAs, (Baumgarten et al., 2013; Lin et al., 2015), and/or RNA-editing (Liew et al., 2017) differential expression may not necessarily be observed.

Conclusions

In this study, we examined developmental sensitivity to and phenotypic consequences of OA during and after the MZT in the rice coral, *Montipora capitata*. While on a transcriptomic level, no differential gene expression was observed in the host until after the MZT, phenotypically, early gastrula (14 hpf) and swimming larvae developing in the pH 7.6 and pH 7.3 treatments were significantly smaller than those in the control pH 7.8. This supports that the development of *M. capitata* embryos is resilient to low pH conditions, even those substantially lower than what currently occurs in Kāneʻohe Bay. While the MTZ appears to be robust to OA, the energetic strain on larvae from maintaining homeostasis under low pH could create negative carryover effects for the energetically costly process of metamorphosis (Edmunds et al., 2013) and may make recruits more susceptible to competition and predation (Anlauf et al., 2011; Pechenik et al., 2002; Thiyagarajan et al., 2007). Lowered fitness in these early life stages could potentially create an ontogenetic bottleneck that impacts the repopulation and replenishment of coral reefs and contribute to their continued decline (Hughes and Tanner, 2000). Of note, however, the reductions in body size detected so far in coral larvae represent the effects of future OA conditions on modern populations without consideration of potential moderating effects of rapid adaptation or acclimatization, which is pivotal to accurately forecast the impacts of climate change on marine organisms (Kelly et al., 2013; Putnam, 2021).

Acknowledgements

We would like to extend our gratitude to the faculty and staff of the Hawaiʻi Institute of Marine Biology and the University of Rhode Island Computing for accommodating us and for their technical support.

Competing Interests

We declare no competing interests.

Funding

This work was funded by BSF grant 2016321 to HMP and TM. This work was also partially supported by the USDA National Institute of Food and Agriculture, Hatch Formula project accession number 1017848.

Data Availability

All raw data can be accessed on the NCBI SRA repository under the Bioproject accession IDs, PRJNA731596 (adult) and PRJNA616341 (all other timepoints). Additionally, all scripts used for bioinformatic and statistical analyses are available on the GitHub repository, Mcapitata_OA_Developmental_Gene_Expression_Timeseries.

References

Adjeroud, M., Kayal, M. and Penin, L. (2017). Importance of Recruitment Processes in the Dynamics and Resilience of Coral Reef Assemblages. *Marine Animal Forests* 549–569.

Albright, R. (2011). Reviewing the Effects of Ocean Acidification on Sexual Reproduction and Early Life History Stages of Reef-Building Corals. *J. Mar. Biol.* **2011**, 1–14.

Albright, R. and Langdon, C. (2011). Ocean acidification impacts multiple early life history processes of the Caribbean coral Porites astreoides: OCEAN ACIDIFICATION IMPACTS CORAL RECRUITMENT. *Glob. Chang. Biol.* **17**, 2478–2487.

Albright, R. and Mason, B. (2013). Projected near-future levels of temperature and pCO2 reduce coral fertilization success. *PLoS One* **8**, e56468.

Albright, R., Mason, B. and Langdon, C. (2008). Effect of aragonite saturation state on settlement and post-settlement growth of Porites astreoides larvae. *Coral Reefs* **27**, 485–490.

Albright, R., Mason, B., Miller, M. and Langdon, C. (2010). Ocean acidification compromises recruitment success of the threatened Caribbean coral Acropora palmata. *Proc. Natl. Acad. Sci. U. S. A.* **107**, 20400–20404.

Altschul, S. F., Madden, T. L., Schäffer, A. A., Zhang, J., Zhang, Z., Miller, W. and Lipman, D. J. (1997). Gapped BLAST and PSI-BLAST: a new generation of protein database search programs. *Nucleic Acids Res.* **25**, 3389–3402.

Anlauf, H., D'Croz, L. and O'Dea, A. (2011). A corrosive concoction: The combined effects of ocean warming and acidification on the early growth of a stony coral are multiplicative. *J. Exp. Mar. Bio. Ecol.* **397**, 13–20.

Aramaki, T., Blanc-Mathieu, R., Endo, H., Ohkubo, K., Kanehisa, M., Goto, S. and Ogata, H. (2020). KofamKOALA: KEGG Ortholog assignment based on profile HMM and adaptive score threshold. *Bioinformatics* **36**, 2251–2252.

Ashburner, M., Ball, C. A., Blake, J. A., Botstein, D., Butler, H., Cherry, J. M., Davis, A. P., Dolinski, K., Dwight, S. S., Eppig, J. T., et al. (2000). Gene ontology: tool for the unification of biology. The Gene Ontology Consortium. *Nat. Genet.* **25**, 25–29.

Barros, P., Sobral, P., Range, P., Chícharo, L. and Matias, D. (2013). Effects of sea-water acidification on fertilization and larval development of the oyster Crassostrea gigas. *J. Exp. Mar. Bio. Ecol.* **440**, 200–206.

Barton, A., Hales, B., Waldbusser, G. G., Langdon, C. and Feely, R. A. (2012). The Pacific oyster,Crassostrea gigas, shows negative correlation to naturally elevated carbon dioxide levels: Implications for near-term ocean acidification effects. *Limnol. Oceanogr.* **57**, 698–710.

Bindoff, N. L., Cheung, W. W. L., Kairo, J. G., Arístegui, J., Guinder, V. A., Hallberg, R., Hilmi, N. J. M., Jiao, N., Karim, M. S., Levin, L., et al. (2019). Changing Ocean, Marine Ecosystems, and Dependent Communities. In (ed. Pörtner, H.-O.), Roberts, D. C.), Masson-Delmotte, V.), Zhai, P.), Tignor, M.), Poloczanska, E.), Mintenbeck, K.), Alegría, A.), Nicolai, M.), Okem, A.), et al.), pp. 477–587. Switzerland: Intergovernmental Panel on Climate Change.

Björklund, M. (2019). Cell size homeostasis: Metabolic control of growth and cell division. *Biochim. Biophys. Acta Mol. Cell Res.* **1866**, 409–417.

Byrne, M. (2012). Global change ecotoxicology: Identification of early life history bottlenecks in marine invertebrates, variable species responses and variable experimental approaches. *Mar. Environ. Res.* **76**, 3–15.

Byrne, M. and Przeslawski, R. (2013). Multistressor impacts of warming and acidification of the ocean on marine invertebrates' life histories. *Integr. Comp. Biol.* **53**, 582–596.

Byrne, M., Ho, M., Selvakumaraswamy, P., Nguyen, H. D., Dworjanyn, S. A. and Davis, A. R. (2009). Temperature, but not pH, compromises sea urchin fertilization and early development under near-future climate change scenarios. *Proc. Biol. Sci.* **276**, 1883–1888.

Caldeira, K. and Wickett, M. E. (2003). Oceanography: anthropogenic carbon and ocean pH. *Nature* **425**, 365.

Chen, H. and Boutros, P. C. (2011). VennDiagram: a package for the generation of highly-customizable Venn and Euler diagrams in R. *BMC Bioinformatics* **12**, 35.

Chille, E. E., Strand, E., Neder, M., Schmidt, V., Sherman, M., Putnam, H. M. and Mass, T. (2021). Developmental series of gene expression clarifies maternal mRNA provisioning and maternal-to-zygotic transition in the reef-building coral Montipora capitata. *bioRxiv* 2021.04.14.439692.

Chua, C. M., Leggat, W., Moya, A. and Baird, A. H. (2013a). Temperature affects the early life history stages of corals more than near future ocean acidification. *Mar. Ecol. Prog. Ser.* **475**, 85–92.

Chua, C. M., Leggat, W., Moya, A. and Baird, A. H. (2013b). Near-future reductions in pH will have no consistent ecological effects on the early life-history stages of reef corals. *Mar. Ecol. Prog. Ser.* **486**, 143–151.

Dahlke, F. T., Leo, E., Mark, F. C., Pörtner, H.-O., Bickmeyer, U., Frickenhaus, S. and Storch, D. (2017). Effects of ocean acidification increase embryonic sensitivity to thermal extremes in Atlantic cod, Gadus morhua. *Glob. Chang. Biol.* **23**, 1499–1510.

Dahlke, F. T., Lucassen, M., Bickmeyer, U., Wohlrab, S., Puvanendran, V., Mortensen, A., Chierici, M., Pörtner, H.-O. and Storch, D. (2020). Fish embryo vulnerability to combined acidification and warming coincides with a low capacity for homeostatic regulation. *J. Exp. Biol.* **223**,.

DeSalvo, M. K., Voolstra, C. R., Sunagawa, S., Schwarz, J. A., Stillman, J. H., Coffroth, M. A., Szmant, A. M. and Medina, M. (2008). Differential gene expression during thermal stress and bleaching in the Caribbean coral Montastraea faveolata. *Mol. Ecol.* **17**, 3952–3971.

DeSalvo, M. K., Sunagawa, S., Voolstra, C. R. and Medina, M. (2010). Transcriptomic responses to heat stress and bleaching in the elkhorn coral Acropora palmata. *Mar. Ecol. Prog. Ser.* **402**, 97–113.

Dickson, A. G. (1990). Standard potential of the reaction: AgCl(s) + 12H2(g) = Ag(s) + HCl(aq), and and the standard acidity constant of the ion HSO4− in synthetic sea water from 273.15 to 318.15 K. *J. Chem. Thermodyn.* **22**, 113–127.

Dickson, A. G., Sabine, C. L. and Christian, J. R. (2007). *Guide to best practices for ocean CO2 measurements*. North Pacific Marine Science Organization.

Doney, S. C., Fabry, V. J., Feely, R. A. and Kleypas, J. A. (2009). Ocean acidification: the other CO2 problem. *Ann. Rev. Mar. Sci.* **1**, 169–192.

Drupp, P., De Carlo, E. H., Mackenzie, F. T., Bienfang, P. and Sabine, C. L. (2011). Nutrient Inputs, Phytoplankton Response, and CO2 Variations in a Semi-Enclosed Subtropical Embayment, Kaneohe Bay, Hawaii. *Aquat. Geochem.* **17**, 473–498.

Edmunds, P. J., Cumbo, V. R. and Fan, T.-Y. (2013). Metabolic costs of larval settlement and metamorphosis in the coral Seriatopora caliendrum under ambient and elevated pCO2. *J. Exp. Mar. Bio. Ecol.* **443**, 33–38.

Ericson, J. A., Lamare, M. D., Morley, S. A. and Barker, M. F. (2010). The response of two ecologically important Antarctic invertebrates (Sterechinus neumayeri and Parborlasia corrugatus) to reduced seawater pH: effects on fertilisation and embryonic development. *Mar. Biol.* **157**, 2689–2702.

Ericson, J. A., Ho, M. A., Miskelly, A., King, C. K. and Virtue, P. (2012). Combined effects of two ocean change stressors, warming and acidification, on fertilization and early development of the Antarctic echinoid Sterechinus …. *Polar Biol.*

Fernandes, P. N., Mannarino, S. C., Silva, C. G., Pereira, M. D., Panek, A. D. and Eleutherio, E. C. A. (2007). Oxidative stress response in eukaryotes: effect of glutathione, superoxide dismutase and catalase on adaptation to peroxide and menadione stresses inSaccharomyces cerevisiae. *Redox Report* **12**, 236–244.

Foo, S. A., Dworjanyn, S. A., Poore, A. G. B. and Byrne, M. (2012). Adaptive capacity of the habitat modifying sea urchin Centrostephanus rodgersii to ocean warming and ocean acidification: performance of early embryos. *PLoS One* **7**, e42497.

Fuchs, Y. and Steller, H. (2015). Live to die another way: modes of programmed cell death and the signals emanating from dying cells. *Nat. Rev. Mol. Cell Biol.* **16**, 329–344.

Gattuso, J.-P., Epitalon, J.-M., Lavigne, H., Orr, J., Gentili, B., Hofmann, A., Proye, A., Soetaert, K. and Rae, J. (2015). seacarb: Seawater carbonate chemistry. *R package version* **3**,.

Gazeau, F., Gattuso, J.-P., Dawber, C., Pronker, A. E., Peene, F., Peene, J., Heip, C. H. R. and Middelburg, J. J. (2010). Effect of ocean acidification on the early life stages of the blue mussel Mytilus edulis. *Biogeosciences* **7**, 2051–2060.

Gentleman, R., Carey, V., Huber, W. and Hahne, F. (2020). *genefilter: genefilter: methods for filtering genes from high-throughput experiments*.

Gibbin, E. M., Putnam, H. M., Davy, S. K. and Gates, R. D. (2014). Intracellular pH and its response to CO2-driven seawater acidification in symbiotic versus non-symbiotic coral cells. *J. Exp. Biol.* **217**, 1963–1969.

Grabherr, M. G., Haas, B. J., Yassour, M., Levin, J. Z., Thompson, D. A., Amit, I., Adiconis, X., Fan, L., Raychowdhury, R., Zeng, Q., et al. (2011). Full-length transcriptome assembly from RNA-Seq data without a reference genome. *Nat. Biotechnol.* **29**, 644–652.

Gu, Z., Eils, R. and Schlesner, M. (2016). Complex heatmaps reveal patterns and correlations in multidimensional genomic data. *Bioinformatics* **32**, 2847–2849.

Guillermic, M., Cameron, L. P., De Corte, I., Misra, S., Bijma, J., de Beer, D., Reymond, C. E., Westphal, H., Ries, J. B. and Eagle, R. A. (2021). Thermal stress reduces pocilloporid coral resilience to ocean acidification by impairing control over calcifying fluid chemistry. *Sci Adv* **7**,.

Hamdoun, A. and Epel, D. (2007). Embryo stability and vulnerability in an always changing world. *Proc. Natl. Acad. Sci. U. S. A.* **104**, 1745–1750.

Han, Y., Shi, W., Tang, Y., Zhao, X., Du, X., Sun, S., Zhou, W. and Liu, G. (2021). Ocean acidification increases polyspermy of a broadcast spawning bivalve species by hampering membrane depolarization and cortical granule exocytosis. *Aquat. Toxicol.* **231**, 105740.

Harii, S., Yamamoto, M. and Hoegh-Guldberg, O. (2010). The relative contribution of dinoflagellate photosynthesis and stored lipids to the survivorship of symbiotic larvae of the reef-building corals. *Mar. Biol.* **157**, 1215–1224.

Harvell, C. D., Mitchell, C. E., Ward, J. R., Altizer, S., Dobson, A. P., Ostfeld, R. S. and Samuel, M. D. (2002). Climate warming and disease risks for terrestrial and marine biota. *Science* **296**, 2158–2162.

Havenhand, J. N., Buttler, F.-R., Thorndyke, M. C. and Williamson, J. E. (2008). Near-future levels of ocean acidification reduce fertilization success in a sea urchin. *Curr. Biol.* **18**, R651–R652.

Helm, R. R., Siebert, S., Tulin, S., Smith, J. and Dunn, C. W. (2013). Characterization of differential transcript abundance through time during Nematostella vectensis development. *BMC Genomics* **14**, 266.

Heyward, AJ (1986). Sexual reproduction in five species of the coral Montipora. *Hawaii Institute of Marine Biology, Technical Report* **37**, 170–178.

Hughes, T. P. and Tanner, J. E. (2000). Recruitment failure, life histories, and long-term decline of Caribbean corals. *Ecology* **81**, 2250–2263.

Hughes, T. P., Barnes, M. L., Bellwood, D. R., Cinner, J. E., Cumming, G. S., Jackson, J. B. C., Kleypas, J., van de Leemput, I. A., Lough, J. M., Morrison, T. H., et al. (2017). Coral reefs in the Anthropocene. *Nature* **546**, 82–90.

Jury, C. P., Thomas, F. I. M., Atkinson, M. J. and Toonen, R. J. (2013). Buffer Capacity, Ecosystem Feedbacks, and Seawater Chemistry under Global Change. *Water* **5**, 1303–1325.

Kaniewska, P., Campbell, P. R., Kline, D. I., Rodriguez-Lanetty, M., Miller, D. J., Dove, S. and Hoegh-Guldberg, O. (2012). Major cellular and physiological impacts of ocean acidification on a reef building coral. *PLoS One* **7**, e34659.

Kelly, M. W., Padilla-Gamiño, J. L. and Hofmann, G. E. (2013). Natural variation and the capacity to adapt to ocean acidification in the keystone sea urchin Strongylocentrotus purpuratus. *Glob. Chang. Biol.* **19**, 2536–2546.

Kim, D., Paggi, J. M., Park, C., Bennett, C. and Salzberg, S. L. (2019). Graph-based genome alignment and genotyping with HISAT2 and HISAT-genotype. *Nat. Biotechnol.* **37**, 907–915.

Krief, S., Hendy, E. J., Fine, M., Yam, R., Meibom, A., Foster, G. L. and Shemesh, A. (2010). Physiological and isotopic responses of scleractinian corals to ocean acidification. *Geochim. Cosmochim. Acta* **74**, 4988–5001.

Kroeker, K. J., Kordas, R. L., Crim, R. N. and Singh, G. G. (2010). Meta-analysis reveals negative yet variable effects of ocean acidification on marine organisms. *Ecol. Lett.* **13**, 1419–1434.

Kurihara, H. and Shirayama, Y. (2004). Effects of increased atmospheric CO on sea urchin early development. *V ol.* **274**, 161–169.

Langmead, B. (2010). Aligning short sequencing reads with Bowtie. *Curr. Protoc. Bioinformatics* **Chapter 11**, Unit 11.7.

Lesser, M. P. and Farrell, J. H. (2004). Exposure to solar radiation increases damage to both host tissues and algal symbionts of corals during thermal stress. *Coral Reefs* **23**, 367–377.

Li, B. and Dewey, C. N. (2011). RSEM: accurate transcript quantification from RNA-Seq data with or without a reference genome. *BMC Bioinformatics* **12**, 323.

Liew, Y. J., Aranda, M. and Voolstra, C. R. (2016). Reefgenomics.Org - a repository for marine genomics data. *Database* **2016**, baw152.

Liew, Y. J., Zoccola, D., Li, Y., Tambutté, E., Venn, A. A., Michell, C. T., Cui, G., Deutekom, E. S., Kaandorp, J. A., Voolstra, C. R., et al. (2018). Epigenome-associated phenotypic acclimatization to ocean acidification in a reef-building coral. *Sci Adv* **4**, eaar8028.

Linkermann, A. and Green, D. R. (2014). Necroptosis. *N. Engl. J. Med.* **370**, 455–465.

Love, M., Huber, W. and Anders, S. (2014a). Moderated estimation of fold change and dispersion for RNA-seq data with DESeq2. *Genome Biol.* **15**, 550.

Love, M., Anders, S. and Huber, W. (2014b). Differential analysis of count data--the DESeq2 package. *Genome Biol.* **15**, 10–1186.

Lueker, T. J., Dickson, A. G. and Keeling, C. D. (2000). Ocean pCO2 calculated from dissolved inorganic carbon, alkalinity, and equations for K1 and K2: validation based on laboratory measurements of CO2 in gas and seawater at equilibrium. *Mar. Chem.* **70**, 105–119.

Malika, C., Ghazzali, N., Boiteau, V. and Niknafs, A. (2014). NbClust: an R package for determining the relevant number of clusters in a data Set. *J. Stat. Softw.* **61**, 1–36.

Martínez, R. (2007). Effects of ultraviolet radiation on protein content, respiratory electron transport system (ETS) activity and superoxide dismutase (SOD) activity of Antarctic plankton. *Polar Biol.* **30**, 1159–1172.

Maynard, J., Van Hooidonk, R., Eakin, C. M., Puotinen, M., Garren, M., Williams, G., Heron, S. F., Lamb, J., Weil, E., Willis, B., et al. (2015). Projections of climate conditions that increase coral disease susceptibility and pathogen abundance and virulence. *Nat. Clim. Chang.* **5**, 688–694.

Miettinen, T. P. and Björklund, M. (2017). Mitochondrial Function and Cell Size: An Allometric Relationship. *Trends Cell Biol.* **27**, 393–402.

Morita, M., Suwa, R., Iguchi, A., Nakamura, M., Shimada, K., Sakai, K. and Suzuki, A. (2010). Ocean acidification reduces sperm flagellar motility in broadcast spawning reef invertebrates. *Zygote* **18**, 103–107.

Moya, A., Huisman, L., Ball, E. E., Hayward, D. C., Grasso, L. C., Chua, C. M., Woo, H. N.,

Gattuso, J.-P., Forêt, S. and Miller, D. J. (2012). Whole Transcriptome Analysis of the Coral *Acropora millepora* Reveals Complex Responses to CO_2 -driven Acidification during the Initiation of Calcification. *Mol. Ecol.* **21**, 2440–2454.

Moya, A., Huisman, L., Forêt, S., Gattuso, J.-P., Hayward, D. C., Ball, E. E. and Miller, D. J. (2015). Rapid acclimation of juvenile corals to CO_2 -mediated acidification by upregulation of heat shock protein and Bcl-2 genes. *Mol. Ecol.* **24**, 438–452.

Nakamura, M., Ohki, S., Suzuki, A. and Sakai, K. (2011). Coral larvae under ocean acidification: survival, metabolism, and metamorphosis. *PLoS One* **6**, e14521.

O'Donnell, M. J., Todgham, A. E., Sewell, M. A., Hammond, L. M., Ruggiero, K., Fangue, N. A., Zippay, M. L. and Hofmann, G. E. (2010). Ocean acidification alters skeletogenesis and gene expression in larval sea urchins. *Mar. Ecol. Prog. Ser.* **398**, 157–171.

Padilla-Gamiño, J. L. and Gates, R. D. (2012). Spawning dynamics in the Hawaiian reef-building coral Montipora capitata. *Mar. Ecol. Prog. Ser.* **449**, 145–160.

Parker, L. M., Ross, P. M. and O'connor, W. A. (2009). The effect of ocean acidification and temperature on the fertilization and embryonic development of the Sydney rock oysterSaccostrea glomerata(Gould 1850). *Glob. Chang. Biol.* **15**, 2123–2136.

Parker, L. M., Ross, P. M. and O'Connor, W. A. (2010). Comparing the effect of elevated pCO2 and temperature on the fertilization and early development of two species of oysters. *Marine Biology* **157**, 2435–2452.

Pechenik, J. A., Jarrett, J. N. and Rooney, J. (2002). Relationships between larval nutritional experience, larval growth rates, juvenile growth rates, and juvenile feeding rates in the prosobranch gastropod Crepidula fornicata. *Journal of Experimental Marine Biology and Ecology* **280**, 63–78.

Perez, F. F. and Fraga, F. (1987). Association constant of fluoride and hydrogen ions in seawater. *Mar. Chem.* **21**, 161–168.

Pertea, M., Pertea, G. M., Antonescu, C. M., Chang, T.-C., Mendell, J. T. and Salzberg, S. L. (2015). StringTie enables improved reconstruction of a transcriptome from RNA-seq reads. *Nat. Biotechnol.* **33**, 290–295.

Polato, N. R., Altman, N. S. and Baums, I. B. (2013). Variation in the transcriptional response of threatened coral larvae to elevated temperatures. *Mol. Ecol.* **22**, 1366–1382.

Poquita-Du, R. C., Huang, D., Chou, L. M., Mrinalini and Todd, P. A. (2019). Short Term Exposure to Heat and Sediment Triggers Changes in Coral Gene Expression and Photo-Physiological Performance. *Frontiers in Marine Science* **6**,.

Przeslawski, R., Byrne, M. and Mellin, C. (2015). A review and meta-analysis of the effects of multiple abiotic stressors on marine embryos and larvae. *Glob. Chang. Biol.* **21**, 2122–2140.

Putnam, H. M. (2021). Avenues of reef-building coral acclimatization in response to rapid environmental change. *J. Exp. Biol.* **224**,.

Putnam, H. M., Mayfield, A. B., Fan, T. Y., Chen, C. S. and Gates, R. D. (2013). The physiological and molecular responses of larvae from the reef-building coral Pocillopora damicornis exposed to near-future increases in temperature and pCO2. *Mar. Biol.* **160**, 2157–2173.

R Core Team (2013). R: A language and environment for statistical computing.

Reipschläger, A. and Pörtner, H. O. (1996). Metabolic depression during environmental stress: the role of extracellular versus intracellular pH in Sipunculus nudus. *J. Exp. Biol.* **199**, 1801–1807.

Reyes-Bermudez, A., Villar-Briones, A., Ramirez-Portilla, C., Hidaka, M. and Mikheyev, A. S. (2016). Developmental Progression in the Coral Acropora digitifera Is Controlled by Differential Expression of Distinct Regulatory Gene Networks. *Genome Biol. Evol.* **8**, 851–870.

Reynaud, S., Leclercq, N., Romaine-Lioud, S., Ferrier-Pagés, C., Jaubert, J. and Gattuso, J.-P. (2003). Interacting effects of CO2 partial pressure and temperature on photosynthesis and calcification in a scleractinian coral: EFFECTS OF p CO2 AND TEMPERATURE ON CORAL. *Glob. Chang. Biol.* **9**, 1660–1668.

Ritson-Williams, R. and Arnold, S. N. (2009). New perspectives on ecological mechanisms affecting coral recruitment on reefs. *Contributions to the …*.

Rivest, E. B. and Hofmann, G. E. (2014). Responses of the metabolism of the larvae of Pocillopora damicornis to ocean acidification and warming. *PLoS One* **9**, e96172.

Rosic, N., Kaniewska, P., Chan, C.-K. K., Ling, E. Y. S., Edwards, D., Dove, S. and Hoegh-Guldberg, O. (2014). Early transcriptional changes in the reef-building coral Acropora aspera in response to thermal and nutrient stress. *BMC Genomics* **15**, 1052.

RStudio Team (2020). *RStudio: Integrated Development for R*. Boston, MA: RStudio, PBC.

Sabine, C. L., Feely, R. A., Gruber, N., Key, R. M., Lee, K., Bullister, J. L., Wanninkhof, R., Wong, C. S., Wallace, D. W. R., Tilbrook, B., et al. (2004). The oceanic sink for anthropogenic CO2. *Science* **305**, 367–371.

Sampayo, J. N., Olsen, A. and Lithgow, G. J. (2003). Oxidative stress in Caenorhabditis elegans: protective effects of superoxide dismutase/catalase mimetics. *Aging Cell* **2**, 319–326.

Schneider, C. A., Rasband, W. S. and Eliceiri, K. W. (2012). NIH Image to ImageJ: 25 years of image analysis. *Nat. Methods* **9**, 671–675.

Scucchia, F., Malik, A., Zaslansky, P., Putnam, H. M. and Mass, T. (2021a). Combined responses of primary coral polyps and their algal endosymbionts to decreasing seawater pH.

Scucchia, F., Malik, A., Putnam, H. M. and Mass, T. (2021b). Inherent physiological and genetic traits conferring tolerance to ocean acidification in mesophotic corals.

Shaw, E. C., Hamylton, S. M. and Phinn, S. R. (2016). Incorporating benthic community changes into hydrochemical-based projections of coral reef calcium carbonate production under ocean acidification. *Coral Reefs* **35**, 739–750.

Shumaker, A., Putnam, H. M., Qiu, H., Price, D. C., Zelzion, E., Harel, A., Wagner, N. E., Gates, R. D., Yoon, H. S. and Bhattacharya, D. (2019). Genome analysis of the rice coral Montipora capitata. *Sci. Rep.* **9**, 2571.

Simão, F. A., Waterhouse, R. M., Ioannidis, P., Kriventseva, E. V. and Zdobnov, E. M. (2015). BUSCO: assessing genome assembly and annotation completeness with single-copy orthologs. *Bioinformatics* **31**, 3210–3212.

Sokolova, I. M., Frederich, M., Bagwe, R., Lannig, G. and Sukhotin, A. A. (2012). Energy homeostasis as an integrative tool for assessing limits of environmental stress tolerance in aquatic invertebrates. *Mar. Environ. Res.* **79**, 1–15.

Strader, M. E., Aglyamova, G. V. and Matz, M. V. (2018). Molecular characterization of larval development from fertilization to metamorphosis in a reef-building coral. *BMC Genomics* **19**, 17.

Tadros, W. and Lipshitz, H. D. (2009). The maternal-to-zygotic transition: a play in two acts. *Development* **136**, 3033–3042.

Thiyagarajan, V., Pechenik, J. A., Gosselin, L. A. and Qian, P. Y. (2007). Juvenile growth in barnacles: combined effect of delayed metamorphosis and sub-lethal exposure of cyprids to low-salinity stress. *Mar. Ecol. Prog. Ser.* **344**, 173–184.

Timmins-Schiffman, E., O'Donnell, M. J., Friedman, C. S. and Roberts, S. B. (2013). Elevated pCO2 causes developmental delay in early larval Pacific oysters, Crassostrea gigas. *Marine Biology* **160**, 1973–1982.

Todgham, A. E. and Hofmann, G. E. (2009). Transcriptomic response of sea urchin larvae Strongylocentrotus purpuratus to CO2-driven seawater acidification. *J. Exp. Biol.* **212**, 2579–2594.

Tominaga, T. and Barber, D. L. (1998). Na–H Exchange Acts Downstream of RhoA to Regulate Integrin-induced Cell Adhesion and Spreading. *MBoC* **9**, 2287–2303.

Van Colen, C., Debusschere, E., Braeckman, U., Van Gansbeke, D. and Vincx, M. (2012). The early life history of the clam Macoma balthica in a high CO2 world. *PLoS One* **7**, e44655.

van de Water, J. A. J. M., Ainsworth, T. D., Leggat, W., Bourne, D. G., Willis, B. L. and van Oppen, M. J. H. (2015). The coral immune response facilitates protection against microbes during tissue regeneration. *Mol. Ecol.* **24**, 3390–3404.

Van Etten, J., Shumaker, A., Mass, T., Putnam, H. M. and Bhattacharya, D. (2020). Transcriptome analysis provides a blueprint of coral egg and sperm functions. *PeerJ* **8**, e9739.

Vastenhouw, N. L., Cao, W. X. and Lipshitz, H. D. (2019). The maternal-to-zygotic transition revisited. *Development* **146**,.

Voolstra, C., Miller, D., Ragan, M., Hoffmann, A., Hoegh-Guldberg, O., Bourne, D., Ball, E., Ying, H., Foret, S., Takahashi, S., et al. (2015). The ReFuGe 2020 Consortium—using "omics" approaches to explore the adaptability and resilience of coral holobionts to environmental change. *Frontiers in Marine Science* **2**, 68.

Wickham, H. (2011). ggplot2: ggplot2. *Wiley Interdiscip. Rev. Comput. Stat.* **3**, 180–185.

Young, M. D., Wakefield, M. J., Smyth, G. K. and Oshlack, A. (2010). Gene ontology analysis for RNA-seq: accounting for selection bias. *Genome Biol.* **11**, R14.

Yuan, X., Yuan, T., Huang, H., Jiang, L., Zhou, W. and Liu, S. (2018). Elevated CO2 delays the early development of scleractinian coral Acropora gemmifera. *Sci. Rep.* **8**, 2787.

Zhao, X., Ren, X., Zhu, R., Luo, Z. and Ren, B. (2016). Zinc oxide nanoparticles induce oxidative DNA damage and ROS-triggered mitochondria-mediated apoptosis in zebrafish embryos. *Aquat. Toxicol.* **180**, 56–70.

Tables and Figures

Table 1. Descriptive statistics for temperature, salinity, and carbonate chemistry across the 9 days of exposure (mean ± standard error of the mean).

	n	Temp (°C)	Sal (psu)	pH (Total Scale)	TA (μmol kg^{-1})	pCO_2 (μmol kg^{-1})	CO_3^{-2} (μmol kg^{-1})	HCO_3 (μmol kg^{-1})	DIC (μmol kg^{-1})	Aragonite Saturation State
pH 7.8 (Amb)	50	26.67±0.08	34.27±0.02	7.848±0.006	2210.5±5	661.6±12.3	147.5±1.8	1847.4±6.7	2012.8±5.8	2.37±0.03
pH 7.6 (Low)	48	26.61±0.09	34.29±0.02	7.607±0.007	2210.9±9	1238.2±22.6	91.0±1.1	1987.2±8.5	2111.9±8.8	1.46±0.02
pH 7.3 (Xlow)	46	26.65±0.08	34.25±0.02	7.324±0.007	2205.4±3	2491.2±47.3	49.8±0.7	2083.2±3.8	2200.8±4.3	0.80±0.01

Figure 1. Summary of A) experimental design and B) sampling timeline, including example photographs of each life stage. Early life stages were exposed to treatment immediately after fertilization. Size analyses were performed on all life stages starting with Unfertilized Eggs (0 hpf). Gene expression analyses were performed on the samples following fertilization corresponding to fertilized eggs (1 hpf), cleavage (4 hpf), prawn chip (9 hpf), early gastrula (14 hpf) and swimming larvae (planula, 9 dpf).

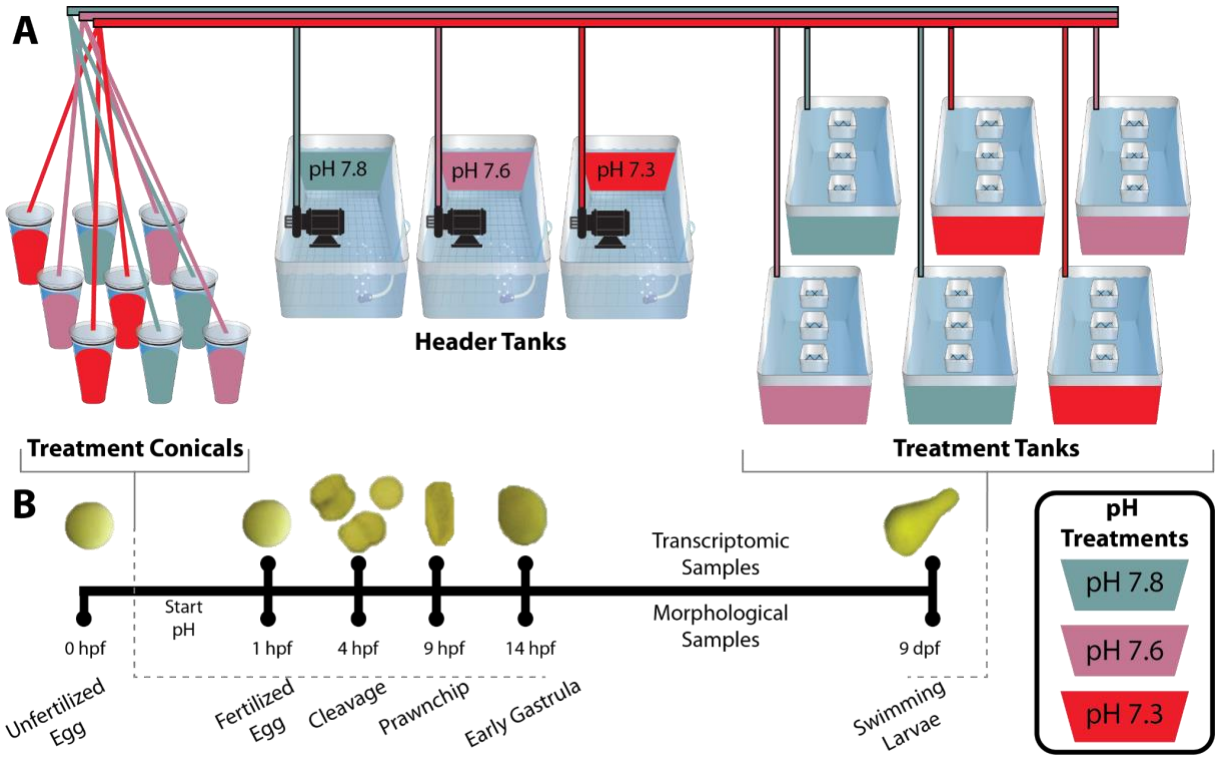

Figure 2. Developmental age and size. A) Proportion of embryos at each cleavage stage at 4 hpf and volume (mm^3) of B) unfertilized eggs, C) fertilized eggs, D) early gastrula, and E) planula in each treatment. Prawn chip stages were not analyzed given the fold in the morphology which generates added assumptions for volume calculations (See Fig. 1 prawn chip picture).

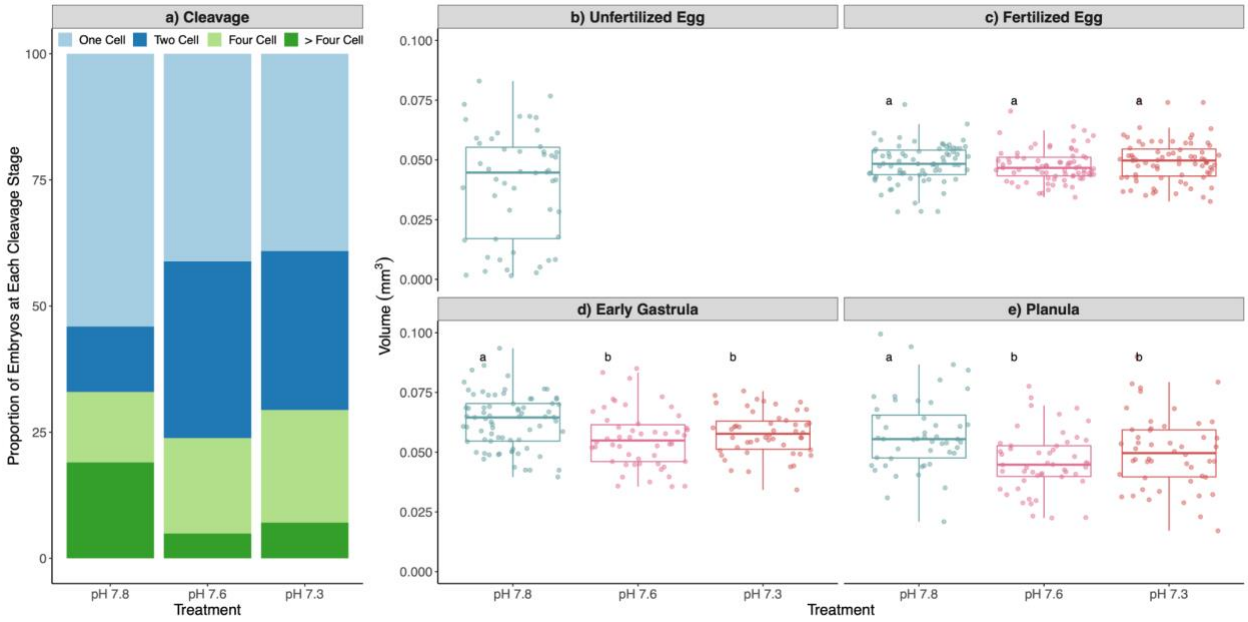

Figure 3. Principal components analyses of sample-to-sample distances based on vst-transformed gene expression. A) principal components analysis of all life stages based on sample-to-sample distance computed from all genes passing a low counts filter, wherein a gene must have a count of 10 or greater in at least 2 out of the 41 samples (pOverA ~0.05, 10). B) shows principal components analysis of the sample-to-sample distance of planula samples, only (pOverA ~0.875, 10).

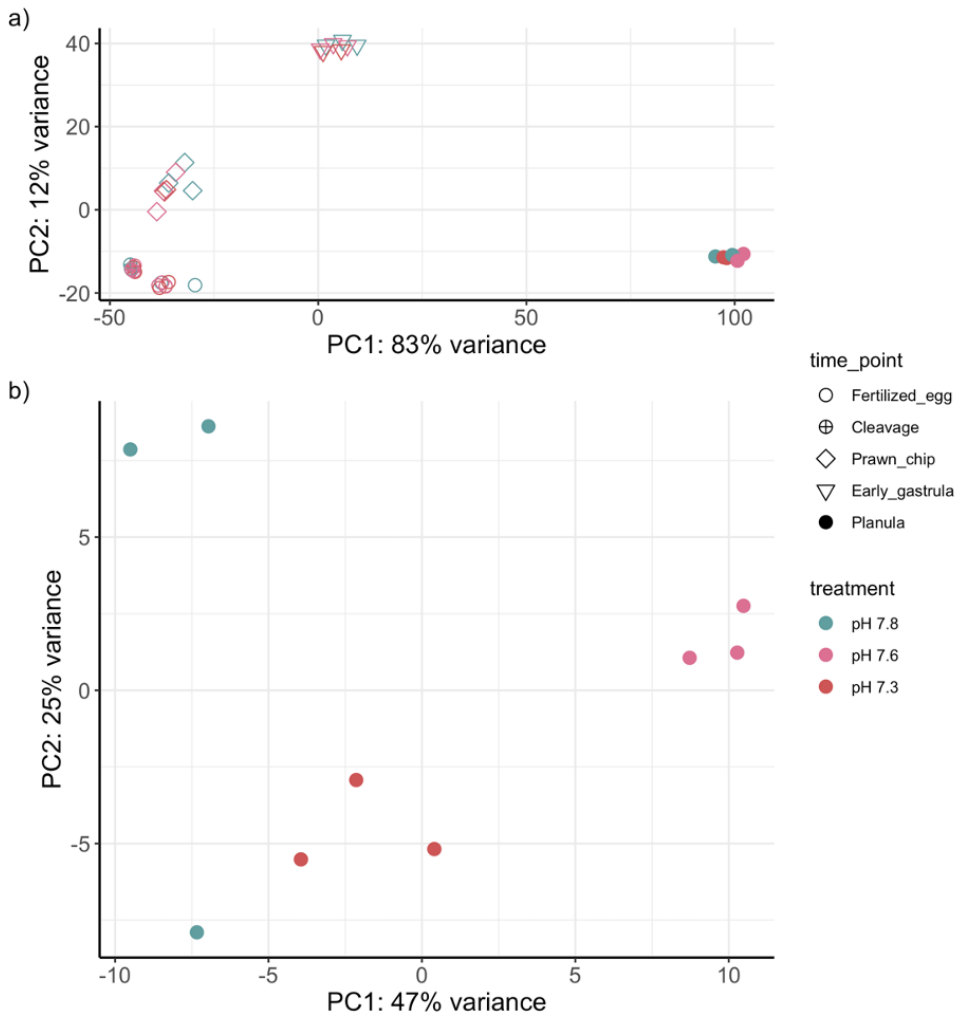

Figure 4. A) Venn diagram and B) heatmap of all genes that are differentially-expressed between treatments at the planula stage. Clusters in the heatmap are based on k-means clustering using the R program NBclust to calculate the optimal number of clusters using 30 indices. Heatmap colors for each gene are based on difference in expression compared to average VST across all samples, where red cells are more highly expressed compared to the rowmean and blue cells more lowly expressed compared to the rowmean.

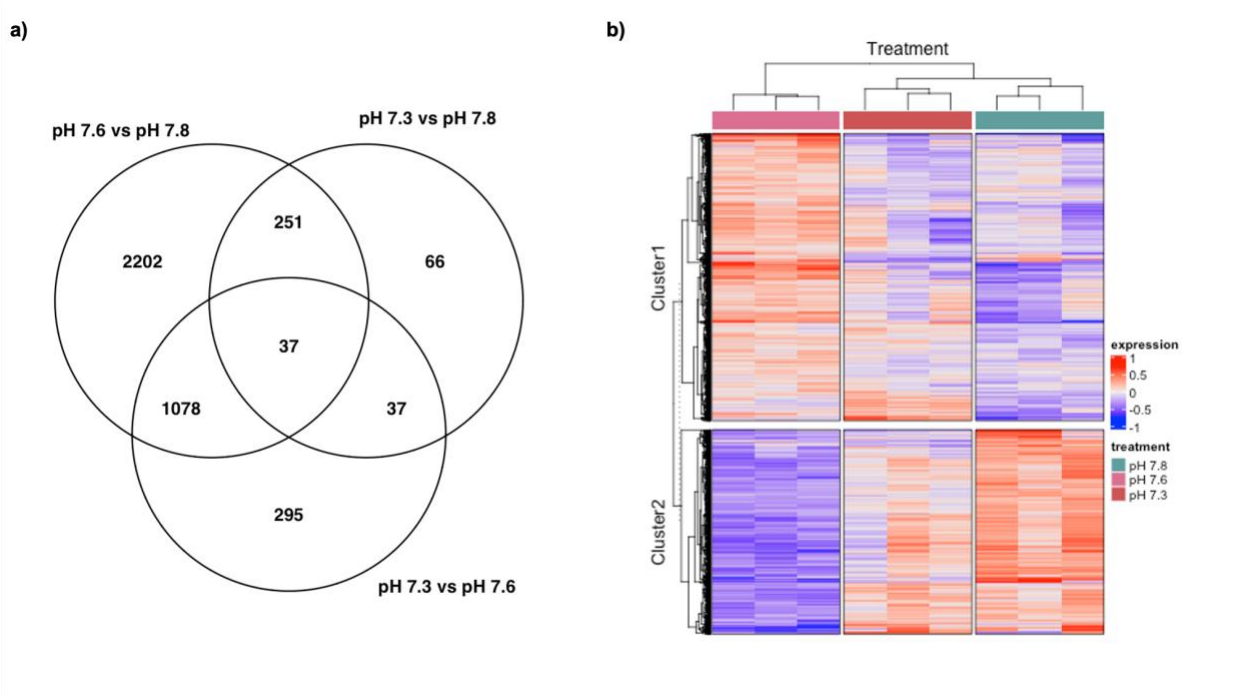

Figure 5. a) Biological process and b) Molecular Function terms that are enriched in planula developing in the low treatment compared to the extreme low and ambient treatments. Up = Terms associated with DEGs (p-adjusted<0.05, log2FoldChange>|1|, numInCat>5) from Cluster 1 (C1), Down = terms associated with DEGs (p-adjusted<0.05, log2FoldChange>|1|, numInCat>5) from Cluster 2 (C2)

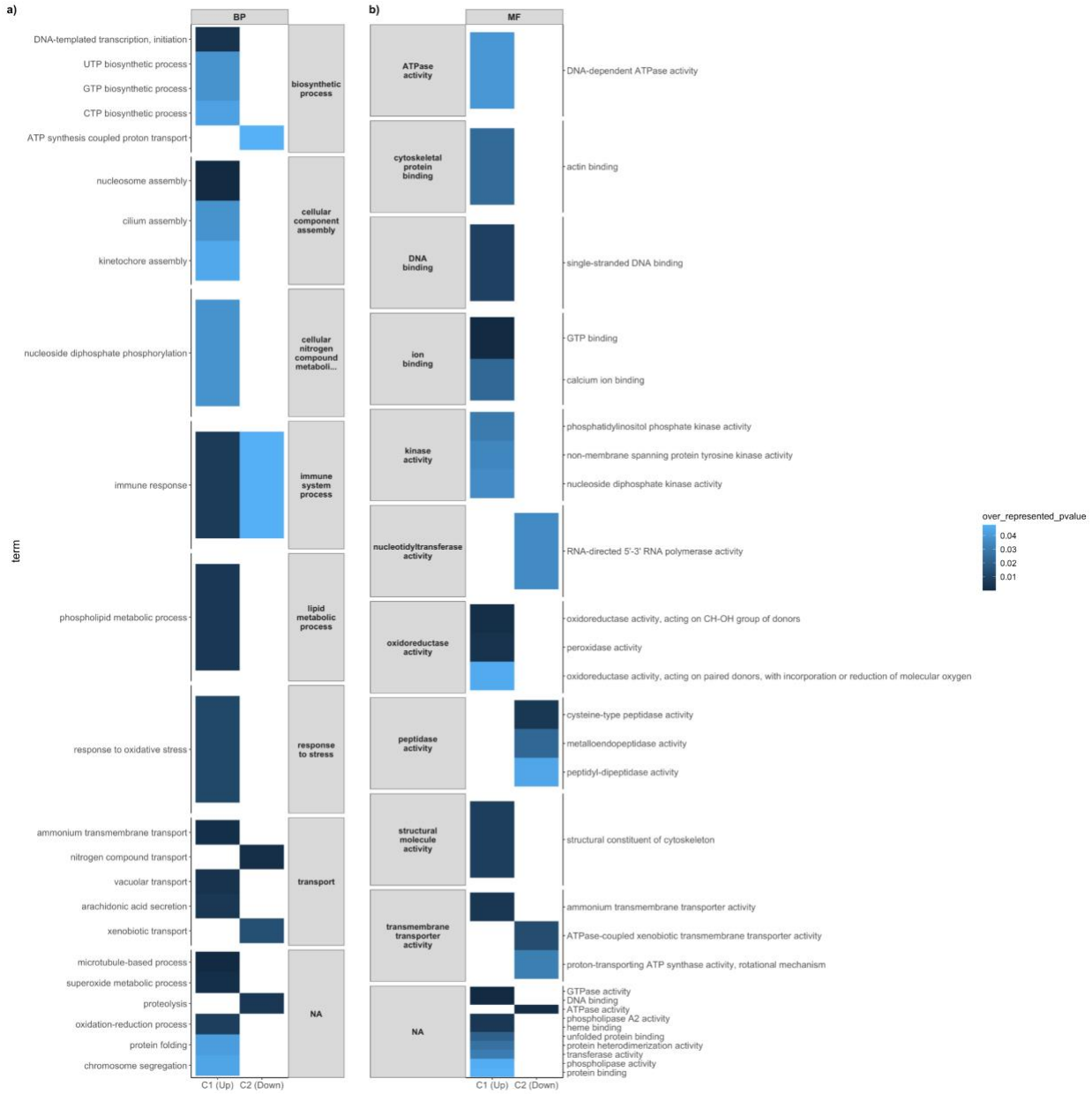

List of Abbreviations

CO_2	carbon dioxide
OA	ocean acidification
MZT	maternal-to-zygotic transition
UV	ultraviolet
ROS	reactive oxygen species
hpf	hours post-fertilization
LPH	liters per hour
dpf	days post-fertilization
vst	variance stabilizing transformation
PCA	principal components analysis
GO	gene ontology
DEG	differentially-expressed gene
PE	paired-end